ANALYSIS OF THE MILKY WAY IN AURIGA

LOIS KIEFER AND ROBERT H. BAKER

SUBMITTED BY
LOIS KIEFER
A.B., Park College, 1935
A.M., University of Illinois, 1938

IN LIEU OF
AN ABSTRACT OF A THESIS
IN PARTIAL FULFILLMENT OF THE REQUIREMENTS
FOR THE DEGREE OF DOCTOR OF PHILOSOPHY IN
MATHEMATICS IN THE GRADUATE SCHOOL OF
THE UNIVERSITY OF ILLINOIS, 1941

Reprinted from
THE ASTROPHYSICAL JOURNAL, Vol. 94, No. 3, November 1941
PRINTED IN THE U.S.A.

ANALYSIS OF THE MILKY WAY IN AURIGA

LOIS KIEFER AND ROBERT H. BAKER

SUBMITTED BY

LOIS KIEFER

A.B., Park College, 1935
A.M., University of Illinois, 1938

IN LIEU OF

AN ABSTRACT OF A THESIS

IN PARTIAL FULFILLMENT OF THE REQUIREMENTS FOR THE DEGREE OF DOCTOR OF PHILOSOPHY IN MATHEMATICS IN THE GRADUATE SCHOOL OF THE UNIVERSITY OF ILLINOIS, 1941

Reprinted from
THE ASTROPHYSICAL JOURNAL, Vol. 94, No. 3, November 1941
PRINTED IN THE U.S.A.

ANALYSIS OF THE MILKY WAY IN AURIGA

LOIS KIEFER AND ROBERT H. BAKER

ABSTRACT

This analysis of the Milky Way to the distance of about 2000 parsecs in the direction of Auriga is based upon counts of stars to the fifteenth magnitude and determination of color excesses of stars in certain latitudes of the region. We find obscuration best represented by two clouds: a very patchy cloud at 300 parsecs, which produces most of the visible bright and dark areas of the region, and a more uniform cloud at 800 parsecs. The density gradients are negative in this direction. Comparisons with other data support, in general, the conclusions of this study.

The region of the Milky Way considered in this paper consists of about 800 square degrees, extending roughly from $+30°$ to $+60°$ in declination and from $3^h\ 30^m$ to $7^h\ 30^m$ in right ascension. In galactic co-ordinates, which are referred to the conventional pole at $+28°$ declination and $12^h\ 40^m$ right ascension, the region lies between longitudes 114° and 146° and latitudes $-7°$ and $+32°$. Centered not far from Capella, the region contains practically all of Auriga and a part of Perseus and includes the galactic anticenter near the eastern boundary. The analysis was made chiefly by Miss Kiefer, who is also responsible for the color determinations. The greater part of the counting was done by Mr. Baker.

THE STAR COUNTS

All the plates used were taken at the University of Illinois Observatory with the 4-inch Ross-Fecker camera, 28 inches in focal length. The scale of the plates is 290″ per millimeter, or about 2° to the inch. The plates used for counts are Cramer Hi-Speed Special.

The region is covered with plates taken in pairs on each of thirty-one centers about 5° apart: one with ten minutes' exposure for counting from magnitude 9 to magnitude 13, and one with sixty minutes' exposure for magnitudes 11–15. A nearly circular area of about 4° radius in the middle of the plate, where the star images are best defined, comprises the countable area. No parts of the plate outside this area are used, either for counting or for calibrating the reference scale. The plates overlap to such an extent that the edge of the countable area on one plate comes nearly to the center of the adjacent plate.

The method of counting the stars and of calibrating the scale is the same as that described in a previous paper.[1] The scale is calibrated for each plate, either directly from catalogued magnitudes of stars in one of the six Selected Areas contained in the region or from sequences of stars measured through overlapping plates from one or more of these Areas. Magnitudes on the International Photographic Scale for Areas 10, 11, 23, 24, 25, and 26 are taken from *Bergedorfer Spektral-Durchmusterung* for stars brighter than magnitude 13 and from the *Mount Wilson Catalogue*[2] for fainter stars. The faintest scale image chosen for counting on any plate is about half a magnitude brighter than the very faintest stars on the plate.

A measure of the consistency of the counts is obtained by comparing counts of the same area on each of four pairs of overlapping plates at centers well scattered over the entire region; the plates of each pair overlap from 12 to 20 square degrees. Table 1 shows the resulting probable errors in log $N(m)$, where $N(m)$ is the number of stars

[1] Baker, *Harvard Circ.*, No. 424, 1939.

[2] *Carnegie Institution of Washington Pub.*, No. 402, 1930.

per square degree brighter than apparent magnitude m. These probable errors are considered satisfactorily small.

The consistency of the magnitude system over the region is examined by comparing the Illinois counts in the Selected Areas with those published in the Bergedorf catalogue for the brighter stars and with the Mount Wilson counts of the fainter stars as tabulated by van Rhijn.[3] The first comparisons involve 81 réseau squares, each 0°.4 on a

TABLE 1

PROBABLE ERRORS OF LOG $N(m)$ FROM OVERLAPPING PLATES

	m						
	9.0	10.0	11.0	12.0	13.0	14.0	15.0
In log $N(m)$.....	±0.02	±0.01	±0.02	±0.02	±0.02	±0.01	±0.01
In magnitude.....	±0.05	±0.02	±0.06	±0.05	±0.07	±0.02	±0.05

TABLE 2

COMPARISON WITH BERGEDORF AND MOUNT WILSON COUNTS

(Illinois *minus* Bergedorf or Mt. Wilson)

	SELECTED AREA						
	10	11	23	24	25	26	Mean
	Δ log $N(m)$						
Berg.							
$9^m.0$.....	−0.09	+0.06	+0.01	−0.06	−0.03	+0.04	−0.01
10.0.....	− .02	− .04	+ .04	− .07	.00	.00	− .01
11.0.....	− .05	− .06	− .03	− .05	+ .02	− .02	− .03
12.0.....	− .11	− .04	− .01	− .01	.00	− .03	− .03
13.0.....	− .11	− .07	− .03	.00	+ .02	+ .01	− .03
Mt. W.							
13.0.....	− .07	− .02	.00	− .09	+ .16	+ .09	+ .01
14.0.....	.00	+ .07	+ .02	+ .02	+ .06	− .11	+ .01
15.0.....	−0.15	+0.15	−0.12	−0.06	−0.06	−0.06	−0.05

side, of our plates and therefore nearly match the areas, 3°.5 on a side, of Bergedorf; the second comparisons involve only 4 squares to correspond more nearly with the Mount Wilson areas, 15′ on a side. The mean differences, in Table 2, appear to be negligible, though the minus sign predominates. In addition, there seems to be no difference between the counts of the two observers and no noticeable effect for either observer, depending on distance from the center of the plate. We have accordingly employed the log $N(m)$ for all the counts without any correction.

In preparation for the analysis the region is divided into areas arbitrarily lettered, in each of which the surface distribution of the stars seems fairly uniform and different

[3] *Groningen Pub.*, **43**, Table 1, 1929.

in density from that of the surrounding divisions. The region is further divided into zones at 2°.5 intervals of galactic latitude. This arrangement is shown in Figure 1 with the omission of the zones from +17°.5 to +30°, throughout each of which the counts are not far from uniform. The most conspicuous bright area, *G*, contains 110 square degrees and extends through four zones; it surrounds the small area *F* in which the

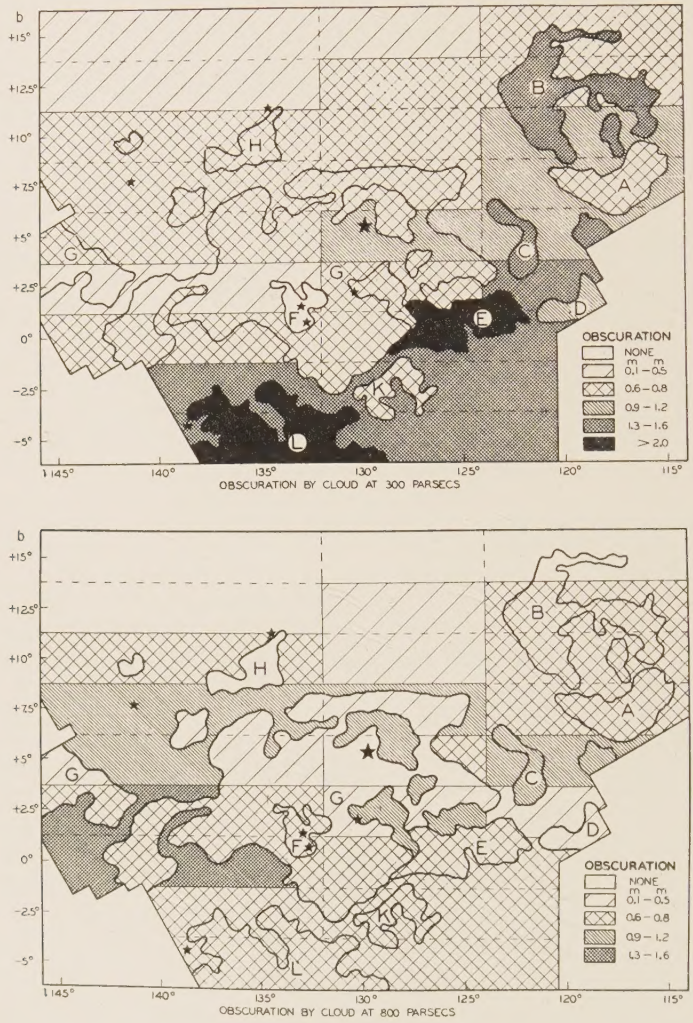

FIG. 1.—Divisions of the Auriga region, showing obscuration at 300 and 800 parsecs

counts run exceptionally high. A succession of four sharply outlined dark areas, *B*, *C*, *E*, and *L*, extends southeastward from the west edge of the region toward the dark clouds of Taurus.

After the bright and dark areas are segregated, the counts in the different zones from latitude +15° to the galactic equator show a significant trend with respect to longitude. In each zone the log $N(m)$ from the separate plates are fairly uniform at longitudes less than 124°, increase from 124° to about 132°, and are again uniform at longitudes

greater than 132°. The increase, which is most conspicuous for the brighter stars, suggests a thinning from west to east of a relatively near-by system of obscuring clouds. Each of these zones is accordingly subdivided for separate analyses into three parts by lines at longitudes 124° and 132°; the latter line is somewhat arbitrarily extended through the $-2\overset{\circ}{.}5$ zone.

Table 3 shows for each division of our region the values of mean log $N(m)$ for magnitudes 9.0–15.0. Before the analysis of the counts is made, these are converted to log $A(m)$ at magnitude intervals from $m = 9.5$ to $m = 14.5$, where $A(m)$ is the number of stars per square degree between $m - \frac{1}{2}$ and $m + \frac{1}{2}$.

THE COLORS

Color excesses of stars from spectral class B8 to class Fo are determined in Selected Areas 10, 25, and 26 and in about 50 square degrees of our areas *G* and *F*, centered in right ascension $5^h\,0^m$, declination $+41\overset{\circ}{.}0$, in order to evaluate the distances of the obscuring clouds and the selective absorption they produce.

Blue magnitudes of the stars were measured on Cramer Hi-Speed Special plates with ten minutes' exposure. The reference scale was similar to that employed in the counting. Red magnitudes were measured on Eastman 103E plates with sixty minutes' exposure behind a ciné-red filter. The star images formed by the Ross-Fecker camera on these excellent plates have so nearly the same appearance as the images on the blue plates that the same reference scale is used for both. Three blue and three red plates were measured in each area. Each blue plate of area *G* and each red plate on all centers was paired with a similar plate of the north polar region taken immediately before or after its mate and similarly exposed and developed.

Photographic-magnitude standards for the Selected Areas are taken from the Bergedorf catalogue, while those for *G* are from the North Polar Sequence.[4] Red-magnitude standards for all areas are taken from the polar-sequence magnitudes determined by C. P. and S. Gaposchkin.[5] Spectra for the Selected Areas are from the Bergedorf catalogue, and those from the area in *G* are from unpublished Harvard Observatory data furnished by Miss Cannon.

Stars from red magnitudes 9 to nearly 13 in spectral classes B8 to Fo are measured in each area. Means of observed blue and red magnitudes are taken for each star. In almost all cases the range in blue or red magnitudes for any star is less than $0\overset{m}{.}3$. No star is used for which the range is as much as $0\overset{m}{.}5$. The stars so excluded are, in general, either very bright or very faint near the limit of the plate.

All stars which appear in any one of the divisions previously determined from the counts are grouped together. Within each group the stars are further divided according to spectral class. For stars of each group the observed color index is plotted against red magnitude. The color excess corresponding to a given red magnitude m is determined from the mean observed color index at m by subtracting the normal color index of the spectral class. Values used as normal color indices are as listed by Bok,[6] extended to include spectral classes A8 to Fo. These values and the corresponding mean absolute magnitudes, $\bar{M}$, from the same source are reproduced in Table 4.

The color excess is converted to photographic absorption, K, on the International Scale by multiplying by the factor 3. This factor 3 is chosen to conform with the practice of others who have used plates of this sort, though slightly better agreement of the analysis for different divisions in the same latitude was found by using the factor 2.5. The mean distance in parsecs from the sun, r, for the group of stars giving each value of K is computed by the formula

$$5 \log r = m - \bar{M} + 5 - K .$$

[4] *Trans. I.A.U.*, 1, 1922. [5] *Harvard Ann.*, **89**, No. 5, 1935. [6] *Ap. J.*, **90**, 249, 1939.

TABLE 3

MEAN LOG $N(m)$ FOR EACH DIVISION

DIVISION	POSITION OF CENTER		AREA (SQUARE DEGREES)	m							TOTAL OBSCURATION (PARSECS)	
	l	b		9.0	10.0	11.0	12.0	13.0	14.0	15.0	300	800
Zone												
+30°0	.....	.....	13	0.35	0.72	1.10	1.48	1.79	2.08	2.35	0^m0	0^m0
+27.5	.....	.....	20	.37	0.74	1.07	1.44	1.78	2.12	2.40	0.0	0.0
+25.0	.....	.....	19	.35	0.72	1.14	1.51	1.86	2.13	2.46	0.0	0.0
+22.5	.....	.....	20	.32	0.73	1.17	1.52	1.86	2.20	2.51	0.0	0.0
+20.0	.....	.....	50	.45	0.80	1.17	1.53	1.87	2.25	2.49	0.0	0.0
+17.5	.....	.....	65	.26	0.70	1.12	1.51	1.88	2.25	2.52	0.0	0.0
+15.0	119°	.....	22	.24	0.62	1.02	1.45	1.76	2.18	2.42	0.8	0.8
+15.0	135	.....	55	.40	0.77	1.16	1.53	1.91	2.30	2.56	0.4	0.4
+12.5	119	.....	20	.28	0.65	1.09	1.42	1.78	2.15	2.41	0.8	1.3
+12.5	128	.....	20	.44	0.79	1.15	1.49	1.88	2.28	2.57	0.5	0.9
+12.5	139	.....	36	.45	0.84	1.26	1.62	2.00	2.39	2.63	0.4	0.4
+10.0	119	.....	18	.20	0.65	1.10	1.40	1.74	2.11	2.39	1.0	1.5
+10.0	128	.....	19	.35	0.72	1.12	1.49	1.85	2.27	2.55	0.8	1.2
+10.0	139	.....	31	.37	0.78	1.23	1.59	1.98	2.36	2.63	0.5	1.0
+ 7.5	119	.....	14	.17	0.60	1.09	1.50	1.85	2.20	2.51	1.0	1.7
+ 7.5	135	.....	38	.41	0.83	1.23	1.60	1.97	2.34	2.62	0.5	1.5
+ 5.0	121	.....	12	.24	0.70	1.16	1.49	1.78	2.12	2.44	1.0	2.2
+ 5.0	128	.....	4	.22	0.71	1.12	1.51	1.89	2.26	2.56	1.0	1.7
+ 5.0	139	.....	15	.44	0.91	1.36	1.73	2.02	2.33	2.63	0.5	1.5
+ 2.5	121	.....	9	.11	0.55	1.00	1.37	1.77	2.14	2.48	1.7	2.0
+ 2.5	128	.....	8	.34	0.78	1.22	1.57	1.94	2.27	2.54	0.9	2.0
+ 2.5	139	.....	9	.38	0.88	1.34	1.75	2.03	2.35	2.63	0.3	1.7
0.0	121	.....	10	.23	0.73	1.13	1.50	1.85	2.20	2.51	1.5	2.1
0.0	139	.....	19	.39	0.86	1.28	1.64	1.96	2.26	2.57	0.7	2.1
− 2.5	125	.....	25	.48	0.79	1.15	1.52	1.86	2.19	2.48	1.3	2.0
− 2.5	137	.....	13	.12	0.53	1.07	1.44	1.80	2.10	2.44	1.5	2.2
− 5.0	125	.....	30	.41	0.78	1.16	1.51	1.85	2.18	2.45	1.2	2.0
Area												
B	120	+15°0	3	.11	0.43	0.93	1.30	1.65	1.92	2.22	1.3	1.3
B	120	+12.5	12	.08	0.52	0.86	1.24	1.57	1.96	2.21	1.5	2.0
B	118	+10.0	9	.32	0.66	0.99	1.30	1.64	1.98	2.24	1.5	2.0
H	135	+10.0	5	.36	0.86	1.29	1.63	2.00	2.45	2.73	0.5	0.5
A	117	+ 7.5	10	.25	0.78	1.21	1.56	1.91	2.26	2.65	0.7	1.5
C	120	+ 5.0	6	.22	0.58	0.96	1.28	1.59	1.93	2.20	1.8	3.0
G	128	+ 7.5	10	.36	0.82	1.24	1.63	2.04	2.41	2.73	0.7	1.0
G	136	+ 7.5	7	.49	0.93	1.34	1.69	2.06	2.44	2.77	0.5	0.9
G	128	+ 5.0	13	.44	0.83	1.26	1.65	2.03	2.43	2.76	0.9	0.9
G	135	+ 5.0	17	.49	0.92	1.40	1.78	2.13	2.47	2.79	0.5	0.8
G	128	+ 2.5	14	.39	0.84	1.30	1.64	1.99	2.38	2.72	0.9	1.2
G	137	+ 2.5	24	.59	1.04	1.49	1.87	2.20	2.52	2.82	0.3	0.8
G	135	0.0	27	.52	0.98	1.42	1.81	2.14	2.47	2.80	0.7	1.2
F	133	+ 2.5	3	.50	0.92	1.56	1.95	2.33	2.66	2.99	0.0	0.5
D	120	+ 2.5	3	.00	0.72	1.18	1.60	2.00	2.39	2.71	0.9	1.2
E	124	0.0	12	.01	0.44	0.84	1.22	1.58	1.96	2.28	2.2	2.8
K	129	− 2.5	5	.59	0.96	1.28	1.64	1.98	2.30	2.63	0.7	1.5
L	132	− 2.5	4	.24	0.48	0.86	1.16	1.50	1.84	2.16	2.5	3.2
L	132	− 5.0	17	0.11	0.39	0.77	1.14	1.48	1.79	2.10	2.5	3.1

The distance and the effectiveness of the obscuring clouds in each division are determined by plotting the values of K against r and drawing the best-fitting curve. The results in four representative areas are shown in Figure 2. Open dots of the graph represent values of K calculated from means of from only four to eight stars and therefore

TABLE 4

ADOPTED NORMAL COLOR INDICES AND MEAN ABSOLUTE MAGNITUDES FOR SPECTRAL CLASSES

Spectral Class	Normal Color Index	Mean Absolute Magnitude, $\bar{M}$
B8–B9	$-0^m.2$	−0.5
A0	− .1	+0.5
A2	.0	+1.5
A3–A7	+ .2	+2.5
A8–F0	+0.3	+3.0

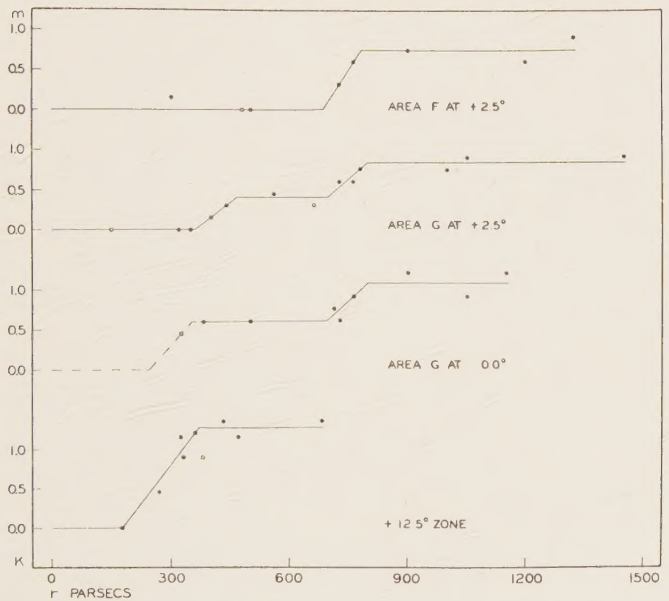

FIG. 2.—Photographic absorption in four divisions of Auriga, determined from color excesses

bear less weight than the solid dots, which represent well-determined absorptions. The data from which points of the graph are determined are listed in Table 5.

The graphs suggest that the absorption is caused by two clouds, one at a mean distance of 300 parsecs, the other at a distance of 800 parsecs. This is supported by the consistency with which obscuration appears at about these distances, with no further obscuration beyond 800 parsecs to the limit of the measurements. The data of the first

three graphs of Figure 2 might also be represented by use of continuous absorption coefficients: $0^m.7$ per kiloparsec, starting at 300 parsecs, for area *F;* $1^m.3$ per kiloparsec, starting at 300 parsecs, for area *G* at $+2°.5$; and $1^m.0$ per kiloparsec for area *G* at 0°. The results of the analyses of the counts made under the two interpretations do not essentially differ. We prefer the two-cloud interpretation because it seems to represent the color determinations more closely, because it gives a somewhat better fit in the analysis of the counts, particularly those of the brighter stars, and because it gives a physical picture.

TABLE 5

ABSORPTION DETERMINED FROM COLORS

Spectral Class	No. of Stars	Mean Red Mag.	Color Excess (Mag.)	Distance (Parsecs)
Area *F* at $+2°.5$				
B8–B9	20	10.5	0.20	1200
	18	11.0	.31	1320
A0–A2	15	10.6	.10	725
	11	11.0	.19	760
	18	11.5	.25	900
A2	6	9.4	.00	480
A3–A7	13	10.0	.05	300
	10	11.0	0.00	500
Area *G* at $+2°.5$				
B8–B9	6	8.9	0.10	660
	8	9.7	.25	780
	19	10.5	.30	1050
	19	11.2	.30	1450
A0	8	9.0	.10	440
	28	10.5	.19	760
	19	11.2	.25	1000
A2	14	9.0	.00	320
	22	10.7	.15	560
	25	11.4	.20	725
A3–A7	25	10.2	.00	350
	33	11.0	.05	400
A8–F0	4	8.9	0.00	150

Spectral Class	No. of Stars	Mean Red Mag.	Color Excess (Mag.)	Distance (Parsecs)
Area *G* at 0°.0				
B8–B9	12	9.4	0.18	725
	15	10.5	.29	1050
	26	11.0	.40	1150
A0	14	10.8	.30	760
	13	11.5	.40	900
A2	5	9.5	.15	325
	15	10.6	.20	500
	26	11.5	.25	710
A3–A7	23	11.0	0.20	380
$+12°.5$ Zone				
B8–A0	5	8.8	0.30	380
	11	10.5	.45	680
A2	11	10.0	.31	330
	10	11.0	.45	430
A3–A7	8	10.0	.15	270
	9	11.2	.38	325
	14	12.0	.38	470
A3–F0	8	9.0	.00	180
A8–F0	8	12.0	0.40	360

There appears to be no obscuration in the $+17°.5$ to $+30°$ zones. Colors in Selected Area 26 show no obscuration in the $+17°.5$ and $+20°$ zones. Hubble's[7] counts of extragalactic nebulae in fields of or adjacent to our region suggest no obscuration in latitudes higher than $+20°$. The mean of two fields in each zone gives $\log N = 1.96$ at $+30°$, 1.60 at $+25°$, and 1.75 at $+20°$, where N is the number of nebulae per field. The mean for the three zones is $\log N = 1.77$, well within the range from 1.60 to 2.22, which Hubble adopts as representing normal distribution of nebulae in the galactic polar caps, where the obscuration must be very little, if any.

Color excesses of some stars and open clusters in certain parts of our region have

[7] *Mt. W. Contr.*, No. 485, 1934.

been measured by other observers. The factors chosen to convert their color excesses to absorption on a scale comparable to our own were determined by the inverse wavelength relation.

The photoelectric survey of the color excesses of class B stars made by Stebbins, Huffer, and Whitford[8] includes a few stars of this region. Their values, multiplied by a factor 7, are compared in Table 6 with our absorption determined from colors in the same divisions. No comparison was attempted in divisions which contained only one star at a suitable distance.

Zug[9] and Cuffey[10] have studied color excesses in a few of the open clusters contained in this region. M37 and M38 appear in Zug's data. Using his distances and converting his color excesses by multiplying by a factor 2.5, we find an absorption of $0^m.4$ at 840 parsecs compared with $0^m.5$ at 300 parsecs and a total of $0^m.8$ at 800 parsecs determined

TABLE 6

COMPARISON WITH STEBBINS, HUFFER, AND WHITFORD

Division	No. of Stars	Distance (Parsecs)	Absorption	
			SHW	Kiefer−SHW
0° zone >132°	5	650	$1^m.0$	$-0^m.3$
+ 2.5 zone >132°	4	1000	1.5	+ .2
F	3	1000	0.3	+ .2
G at +2°.5	6	1000	0.8	.0
+12°.5 zone >132°	2	650	0.2	+0.2

from our colors. Cuffey finds between $1^m.0$ and $2^m.0$ at 900 parsecs for NGC 1893, while we find in the same zone $1^m.2$ at 800 parsecs. He has no obscuration to 600 parsecs for NGC 1857, as compared with $0^m.3$ at 300 parsecs from our colors.

We find in the +7°.5 zone a total absorption of $1^m.5$, which agrees with the results of unpublished measurements in Selected Area 25 kindly supplied by Dr. B. G. Karpov. Thus the agreement of our colors with those of other observers seems generally satisfactory.

ANALYSIS OF THE COUNTS

The analysis is accomplished with the aid of $(m, \log \pi)$ tables whose construction and use have been described by Bok.[11] It is necessary to find for each zone values of $\log A(m)$ representing the counts which would be obtained if the zone were unobscured. Zones from +17°.5 to +30° are apparently unobscured, so the required $A(m)$ are taken directly from the counts. Although no unobscured areas appear in the lower latitudes, the amount and distances of the obscuration in most of the zones are determined from color excesses, and the counts may be corrected to give unobscured values. This is accomplished by introducing in the $(m, \log \pi)$ table of a zone the obscuration determined from colors in a division of that zone and finding a set of factors which produce values of $A(m)$ closely approximating the observed $A(m)$ of the division. This set of factors, representing the density gradient with distance from the sun, is used in computing values of unobscured $A(m)$.

The unobscured $\log A(m)$ were plotted in order of latitude at each magnitude interval

[8] *Mt. W. Contr.*, No. 621, 1940.

[9] *Lick Obs. Bull.*, No. 454, 1933.

[10] *Harvard Ann.*, **105**, No. 21, 1937.

[11] *The Distribution of the Stars in Space*, p. 26, University of Chicago Press, 1937.

from $m = 9.5$ to $m = 14.5$. The resulting graphs are smooth curves with maxima at 0°, which slope uniformly to +17°.5 and then decrease more gradually to +30°. Unobscured log $A(m)$ for +10° and +15° zones were computed from density factors interpolated from those for adjacent zones. Adopted values of unobscured log $A(m)$ for each zone appear in Table 7.

The analysis of the counts in the obscured divisions is made by introducing in the (m, log π) table the amounts of obscuration necessary to make the log $A(m)$, computed from the density gradient of the zone, fit the log $A(m)$ observed for each division. In general, the difference between computed and observed log $A(m)$ is not so great as 0.05. The exact amounts of obscuration determined for each division are given in the last two columns of Table 3.

A picture of the two absorbing clouds is given by the shaded maps of Figure 1. Most of the obscuration is caused by the cloud at 300 parsecs, which extends over the entire

TABLE 7

VALUES OF UNOBSCURED LOG $A(m)$

Zone	m					
	9.5	10.5	11.5	12.5	13.5	14.5
0°.0	1.12	1.52	1.91	2.25	2.54	2.77
2.5	1.02	1.47	1.85	2.21	2.50	2.74
5.0	0.93	1.43	1.80	2.13	2.42	2.68
7.5	0.94	1.39	1.78	2.10	2.41	2.68
10.0	0.84	1.27	1.67	2.01	2.32	2.60
12.5	0.75	1.15	1.53	1.91	2.22	2.46
15.0	0.71	1.09	1.45	1.81	2.05	2.28
17.5	0.56	0.95	1.32	1.66	1.97	2.20
20.0	0.57	0.93	1.32	1.63	1.93	2.15
22.5	0.54	0.91	1.30	1.62	1.91	2.14
25.0	0.50	0.88	1.23	1.56	1.83	2.06
27.5	0.48	0.83	1.20	1.52	1.79	2.04
30 0	0.45	0.83	1.21	1.53	1.75	1.99

region from −5° to +15° with the exception of area F. This near-by cloud, which causes obscuration varying from 0^m.0 to 2^m.5, creates the conspicuous patterns of bright and dark areas shown on the map. Its densest parts form the dark areas B, C, E, and L, and it also outlines the bright areas A, D, F, K and the lower portion of G. The 800-parsec cloud extends from −5° to +12°.5, outlining area H and the upper portion of G. The maximum obscuration of 1^m.4 occurs near the equator in the eastern part of the region.

A number of investigations related to ours have been made in or near our region. Schalén,[12] in his discussion of Auriga, considers parts of areas F, G, and the −2°.5 zone. He combines F and G, since he attributes the difference in brightness to a preponderance of absolutely bright B and A stars in area F. In the −2°.5 zone, Schalén finds a dark cloud beginning at 70 parsecs and extending to 400–500 parsecs with a total obscuration of 1^m.9. We find 1^m.5 at 300 parsecs and a total obscuration of 2^m.2 at 800 parsecs.

Hartwig[13] uses area F as a comparison field for obscured regions in Taurus. He finds 1^m.4 obscuration at a distance of 100–200 parsecs, with a total obscuration of 2^m.1 at 350 parsecs in a region adjacent to our area L where we find an obscuration of 2^m.5 at 300 parsecs. McCuskey's[14] data in Taurus extend to the border of the Auriga region.

[12] *Upsala Medd.*, **55**, 1931.

[13] *Zs. f. Ap.*, **17**, 191, 1939.

[14] *Ap. J.*, **88**, 209, 1938; **89**, 568, 1939.

He finds in the 0°, −2°.5, and −5° zones heavy obscuration caused by a dark cloud at a distance less than 200 parsecs. The dark cloud L is caused by about $2^m.0$ obscuration in McCuskey's analysis and by $2^m.5$ at 300 parsecs in this paper. Our obscurations caused by the near-by cloud run about $0^m.5$ higher than Hartwig's and McCuskey's, which is precisely the amount of obscuration we determined in area F, used by them as an un-

TABLE 8

DENSITY GRADIENTS

Zone	r in Parsecs							
	125	200	300	500	800	1250	2000	3000
0°.0	1.00	1.00	0.90	0.90	0.60	0.30	0.15	0.05
2.5	1.00	1.00	.90	.90	.60	.30	.15	.05
5.0	1.00	1.00	.90	.90	.60	.30	.10	.05
7.5	1.00	1.00	.90	.80	.60	.35	.10	.05
10.0	1.00	1.00	.80	.60	.50	.25	.10	.05
12.5	1.00	0.80	.75	.50	.30	.25	.10	0.02
15.0	1.00	0.80	.75	.50	.25	.15	.05	.....
17.5	1.00	0.75	.50	.30	.20	.10	.07	.....
20.0	1.00	0.75	.50	.30	.20	.10	.05	.....
22.5	1.00	0.70	.50	.30	.20	.09	.05	.....
25.0	1.00	0.60	.40	.30	.20	.09	.02	.....
27.5	1.00	0.60	.40	.25	.15	.10	.02	.....
30.0	1.00	0.60	0.40	0.25	0.15	0.09	0.01	.....

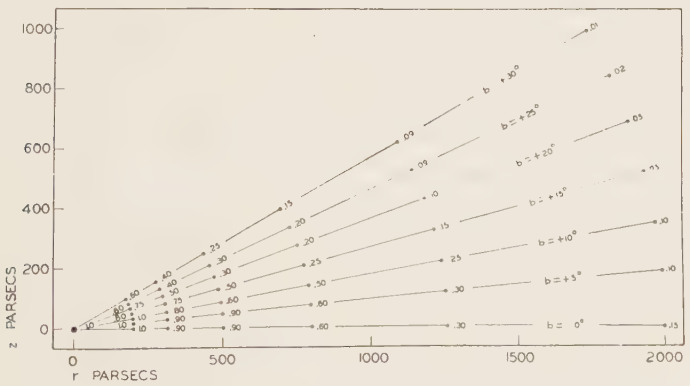

FIG. 3.—Values of density gradients

obscured comparison area. The further obscuration caused by our 800-parsec cloud is balanced by the $0^m.5$-per-kiloparsec continuous absorption coefficient used by McCuskey.

Hubble's[7] counts of extragalactic nebulae indicate an obscuration of $0^m.7$ in the +15° zone as compared with $0^m.4$ from our analysis. Area B at +15° has $1^m.4$ from Hubble's counts and $1^m.3$ from our analysis. Hubble finds, in the +10° zone, $1^m.3$ obscuration at longitudes greater than 132° and $1^m.5$ at longitudes less than 132°; we determine $1^m.0$ and $1^m.5$, respectively for the same regions. For area B at +10° and for all zones closer to the galactic equator Hubble's counts indicate more than $3^m.0$ absorption. We determine from $2^m.1$ to $3^m.1$ obscuration for these zones within the distance of 2000 parsecs from the sun. Additional obscuration may very well be found beyond this distance.

DENSITY GRADIENTS

The adopted density gradients are listed for all zones in Table 8 and are shown in Figure 3 in relation to distance perpendicular to the galactic plane, z, as well as distance from the sun, r. Density was assumed uniform within 200 parsecs of the sun and outside this range is expressed in terms of unit density near the sun. Star densities were considered symmetrical about the galactic equator; those gradients adopted for positive latitudes are also used for the corresponding negative latitudes.

The negative gradients imply that the sun is situated in a region of high density with respect to the direction of Auriga. In the lower latitudes the density is reduced to about one-half at 800 parsecs and to less than one-third at 1200 parsecs from the sun. The negative character of the gradient is not affected when the obscuration is represented by a continuous absorption coefficient. Density factors computed under this hypothesis vary only slightly from the corresponding adopted factors.

Oort[15] has determined density gradients in this region and finds near the galactic equator in the direction of the anticenter a small but well-defined decrease in density factors to 500 parsecs of the sun, then a rise to 1.6 from 870 to 1500 parsecs. An absorption of 2^m5 at a distance less than 800 parsecs would be needed in addition to what we have introduced in the $0°$ to $+5°$ zones in Auriga to bring the $A(m)$ computed from his densities into agreement with the Illinois counts. Such an absorption would not be consistent with our color excesses, which cover this entire range of distances. Accordingly, we conclude that in the direction of Auriga the star density decreases with increasing distance from the sun.

UNIVERSITY OF ILLINOIS OBSERVATORY
August 1941

[15] *B.A.N.*, 308, 1938.

VITA

Lois Kiefer was born in Chicago, Illinois, on April 13, 1915. She received her elementary education in the schools of Kingston, Illinois. She attended Park College, Missouri, from 1931 until receiving the A.B. degree in 1935. Two years, from 1935 to 1937, were spent teaching in the elementary schools of DeKalb County, Illinois. During the summer sessions of 1936 and 1937 and the winter sessions from 1937 to 1941, she attended the University of Illinois. The degree of A.M. in Mathematics was granted by this institution in June, 1938. During the last three and one-half years of attendance at the University of Illinois, she served as an assistant in the Department of Mathematics.